



You have downloaded a document from
RE-BUŚ
repository of the University of Silesia in Katowice

Title: Studying the stability of Solvent Red 19 and 23 as excise duty components under the influence of controlled factors

Author: Michał Daszykowski, Joanna Orzeł, Ivana Stanimirova, Anna Poliwoda, Dorota Pukała, Piotr Młynarz

Citation style: Daszykowski Michał, Orzeł Joanna, Stanimirova Ivana, Poliwoda Anna, Pukała Dorota, Młynarz Piotr. (2020). Studying the stability of Solvent Red 19 and 23 as excise duty components under the influence of controlled factors. "Fuel Processing Technology" (Vol. 206 (2020), Art. No. 106465), doi 10.1016/j.fuproc.2020.106465



Uznanie autorstwa - Licencja ta pozwala na kopiowanie, zmienianie, rozprowadzanie, przedstawianie i wykonywanie utworu jedynie pod warunkiem oznaczenia autorstwa.



UNIwersYTET ŚLĄSKI
W KATOWICACH



Biblioteka
Uniwersytetu Śląskiego



Ministerstwo Nauki
i Szkolnictwa Wyższego



Research article

Studying the stability of Solvent Red 19 and 23 as excise duty components under the influence of controlled factors

M. Daszykowski^{a,*}, J. Orzel^a, I. Stanimirova^a, A. Poliwoda^b, D. Prukala^c, P. Mlynarz^d

^a Institute of Chemistry, University of Silesia in Katowice, 9 Szkolna Street, 40-006 Katowice, Poland

^b Faculty of Chemistry, Opole University, 11a Kopernika Street, 45-040 Opole, Poland

^c Faculty of Chemistry, Adam Mickiewicz University in Poznań, 8 Uniwersytetu Poznańskiego Street, 61-614 Poznań, Poland

^d Department of Chemistry, Wrocław University of Science and Technology, 27 Wybrzeże Wyspiańskiego Street, 50-370 Wrocław, Poland

ARTICLE INFO

Keywords:

Fraud
Fuel laundering
Fuel counterfeiting
Photofading
Lightfastness
Self-sensibilisation

ABSTRACT

In this study, we examine the chemical stability of two disazo dyes, namely Solvent Red 19 and 23 (SR 19 and SR 23), under simulated conditions. Both dyes are considered to be chemically stable under normal exploitation conditions and therefore, are used extensively as excise duty components that enable a rapid visual verification of the tax levels that were imposed on fuel products as well as identifying fuel usage. However, the results from this study confirmed that the colour of the samples that had been fortified with either SR 19 or SR 23 fades under the influence of external conditions such as UV-A irradiation and temperature over time. The UV-A irradiation was the dominant factor that was responsible for the colour of the samples to fade in two designed experiments that were carried out independently for two model systems. The analysis of the UV/Vis and fluorescence spectra as well as the interpretation of the changes that were observed in the chromatographic profiles provided substantial evidence that the colour fading was caused by the photodegradation of the disazo dyes, which also occurs in non-polar media including fuel products. SR 19 is more stable than SR 23.

1. Introduction

Control of fuel products over the stock and their market value stimulates the economy and the development of specific industrial sectors. Depending on the anticipated purpose of usage, e.g. heating, road and marine transport, fueling agricultural machinery, fuel prices are different mostly due to the variations in the tax levels. In many countries, fuel products are tagged with specific chemical substances in order to label the intended purpose of usage [1]. For example, since 2001, the EU regulates the use of an 'invisible' compound, which is known under the name Solvent Yellow 124, as a euromarker for fuel. This euromarker can be detected easily by the police as well as custom and tax officers by performing a simple test outside the laboratory. Besides the addition of the euromarker, fuel products are also spiked with another specific dye, which indicates the intended tax level. Therefore, it is possible to visually confirm the expected purpose of fuel usage and the corresponding tax level. In Poland, fuel products that are designated for heating purposes are tagged with red dyes. These are either Solvent Red 19 or Solvent Red 164 [2], while in the United States of America, Solvent Red 23 (also known as Sudan III) is added to distinguish low-taxed heating oil from automotive diesel fuel. The respective

regulations define the amount of excise duty components (euromarker and dye) in order for the authorized agencies to control their levels easily. Therefore, a decreased concentration of any excise duty component is interpreted as an attempt at fuel counterfeiting.

Illegally removing excise duty components, which is known as 'fuel laundering', is induced by the financial rewards that are expected due to the reduced amounts of rebated tax on fuel products compared to the regular taxes. The effect of this 'laundering' is the loss of fuel colour. Therefore, regulations require that the excise duty components should be (i) difficult to remove at low costs and (ii) chemically stable under normal exploitation conditions. Surprisingly, in practice, these two assumptions are difficult to fulfill, see e.g., [3]. From the chemical point of view, removing the excise duty components from fuel products is not complicated [4–7], while confirming this intentional removal cannot be observed by a simple spectrophotometric assessment of the sample colour [8]. While a lower level than expected of a given dye in a fuel sample can be interpreted as counterfeiting, in practice, it may be observed due to a chemical or photocatalytic degradation that is triggered when a sample is exposed to external factors, among which, UV-A irradiation plays a crucial role, see e.g., [9].

On an everyday basis, the two representatives of the so-called azo

* Corresponding author.

E-mail address: michal.daszykowski@us.edu.pl (M. Daszykowski).

dyes, SR 19 and SR 23, serve as excise duty components. The azo dyes have very vivid colours such as red, orange and blue due to the presence of diaza bond(s) (delocalised π electrons) and chromophore groups in their chemical structures. Delocalised π electrons are responsible for creating some interesting physical and chemical properties. For example, these dyes can easily form different configurational isomers [10] and photoisomerisation is observed due to the changes in the configuration in the functional groups that are attached to the rigid diaza bond(s). These configuration changes are responsible for the changes of the colour in a sample and are especially relevant in our study. Colourfastness, which describes the resistance of the colour of a dye molecule or dyed sample against fading, is another essential property of a dye. Although colourfastness is a fundamental concern in the textile industry, its importance in characterising chemical markers is often neglected. Over the past several years, the photodegradation of azo dyes has been extensively studied [11–13]. Some authors have suggested that the process of photodegradation is driven by the conversion of triplet to singlet oxygen, which is sensibilised by azo compounds. Such a conversion process was proven to be available in azobenzene dyes by Podsiady and Sokolowska [12]. Moreover, the self-sensitised oxidation of an azo dye is significantly delayed when a quencher is added into the system. The authors also noticed that the colour fading of the mixtures that contained azobenzene dyes and their benzothiazolyl analogues was dependent on the configuration of the functional groups and was substantially retarded when the $-N=N-$ group was sterically hindered. They postulated that this process starts with the break of the $-N=N-$ bond. As was described in references [14–16], singlet oxygen plays a crucial role in the process of photochemical degradation, which is not reversible and eventually leads to permanent loss of colour. The formation of singlet oxygen is also promoted by the tautomeric isomerism of azo compounds with the OH- substituent, specifically the presence of a hydrazine tautomer. Such an induction mechanism of photochemical degradation was shown to be true for arylazonaphthols [17]. On the other hand, Morita and Hada questioned the role of azo-hydrazone tautomerism in the photochemical degradation process [16]. They stressed the fact that the intrinsic property of an azo dye molecule to increase its reactivity with self-synthesised singlet oxygen was an essential factor. Various photochemical reactions make the group of azo compounds fascinating and worth exploring. Most of the published studies focus on attempting to find the photochemical reactions that are able to break down the molecules of different industrial azo dyes in an optimal way in order to decrease their presence in the aquatic environment [11,18–20]. One way to do this is via the photocatalytic degradation of industrial dyes using titanium dioxide as the photocatalyst [19,21]. Another possible option for breaking down dye molecules is through a nonselective attack of the hydroxyl- and peroxy-radicals that are generated in the Fenton reaction [22].

In this study, we question the chemical stability of the disazo dyes that are used as excise duty components in the fuel industry and we specify the reasons that are responsible for this instability. The experimental measurements were designed to mimic the behaviour of non-polar fuel samples in order to provide sufficient evidence that SR 19 and SR 23 are unstable in samples that are exposed to UV-A irradiation over time or are stored in high temperatures. The underlying hypothesis is that these factors affect the chemical composition of the model mixtures to a large extent and that the samples would become colourless over time. We are convinced that the qualitative and quantitative data that were obtained from several different analytical techniques will help us to explain the reasons for the limited performance of the spectrophotometric method for determining the amount of excise duty components in fuel products and to determine a possible mechanism for the chemical instability.

As highlighted in the literature, counterfeiting and adulteration of different fuel products is recognized worldwide and considered as a serious issue. Therefore, to date, different analytical methods [23] and advanced approaches extended with chemometric data modeling were

proposed to deal with the identification of possible aspects of fuel counterfeiting, e.g. [24–29] and determining the level excise duty components, e.g. [30].

2. Material and methods

2.1. Design of the experiments

The design of experiments (DoE) is an objective statistical approach that aims to facilitate the planning of an experiment and to further optimise it [31]. In particular, the DoE methods enable the effects of a few external factors to be assessed simultaneously and running a limited number of necessary experiments. In order to evaluate the effect of three external factors such as exposure to UV-A irradiation (A), temperature (B) and the duration of sample storage (C), the experiment was conducted following the full factorial design in which each of the three factors was evaluated at two levels [31]. The samples that were irradiated were placed in quartz flasks and sealed with quartz corks, whereas the samples that were stored in darkness were placed in glass flasks, sealed and carefully covered with thick aluminum sheets. Then, for 64 days, all of the samples were incubated in two climatic chambers (MK 240 and KB 240, Binder) at two different temperatures with or without UV-A irradiation exposure. The climatic chambers permit precise and automatic temperature control over time. The temperature in the chambers was kept at two different (6 °C and 30 °C) but constant levels (the maximal expected temperature fluctuation inside each climatic chamber during the entire experiment was equal to 0.5 °C). In addition, both climatic chambers were equipped with customised illumination panels with five 15 W fluorescent lamps (Actinic BL TL-D, Philips) that generate illumination from the UV-A spectral range with a maximum intensity of between 350 and 400 nm. These two climatic chambers and their possible settings enabled us to study the effect of three different factors (UV-A irradiation, temperature and the duration of sample storage) on the colour intensity of the samples simultaneously, which is in agreement with the principals of experimental design. The colourfastness of the samples was quantified after 17 and 64 days using a UV/Vis spectroscopy and the high-performance liquid chromatography with the UV/Vis detection and mass spectrometry.

2.2. Preparing the model mixtures of Solvent Red 19 and Solvent Red 23

Two separate model mixtures that contained either SR 19 (Sigma-Aldrich, melting point: 130 °C) or SR 23 (Sigma-Aldrich, melting point: 199 °C) were prepared in the following manner. A 3.22 mg of red disazo dye was dissolved in 0.7 dm³ of heptane (Sigma-Aldrich, purity higher than 99%, HPLC grade), which led to a concentration of 4.6 mg·dm⁻³ of dye in the model mixtures.

2.3. UV/Vis measurements

The UV/Vis spectra of the mixtures that contained either SR 19 or SR 23 as a major component were measured using a spectrophotometer Nicolet Evolution 220 LC (Thermo Scientific) coupled with a Peltier thermostatted cell holder to record the spectra at a constant temperature. The spectra were measured in the spectral range of 200 and 1000 nm every 2 nm (the acquisition rate: 1200 nm·min⁻¹ and the integration time: 0.05 s) at 25 °C using standard quartz cuvettes with a 10 nm long optical path.

2.4. Fluorescence excitation-emission measurements

The fluorescence excitation-emission spectra were measured using a Cary Eclipse Fluorescence Spectrophotometer (Varian) equipped with an Agilent Carry Temperature Controller. They were recorded at 25 °C using the Peltier thermostatted multicell holder (possible temperature variation \pm 0.05 °C) for the samples in the standard quartz cuvettes

(optical path length of 10 nm). The following settings of the fluorimeter were used: acquisition rate $1200 \text{ nm}\cdot\text{min}^{-1}$, integration time 0.1 s, detector voltage 600 V and the slit for measuring the excitation and the emission spectra 5 nm. The excitation and emission spectra of the samples that contained SR 19 were collected in the spectral range of 230–360 nm every 10 nm and 280–650 nm with an increment of 2 nm, respectively. The excitation and emission spectra of the samples that contained SR 23 were recorded in the spectral range of 230–400 nm every 10 nm and 250–650 nm every 2 nm, respectively. The Rayleigh and Raman scattering were removed from the excitation-emission spectra using the method described in reference [32] and implemented in Matlab.

2.5. High-performance liquid chromatography

Samples of 1 ml, which contained either SR 19 or SR 23, were concentrated under a nitrogen gas stream. Then, the residues were dissolved in 200 μl of CH_3CN and separated using a Thermo UltiMate 3000 UHPLC-UV (Sunnyvale, CA, USA) system coupled to a micrOTOF-QII mass spectrometer (Bruker Daltonics, Germany) and equipped with an electrospray ionisation source (ESI). Chromatographic separation was performed on an Acclaim RSLC 120 C18 column (2.2 μm , $2.1 \times 100 \text{ mm}$), thermostatted (30 $^\circ\text{C}$) and protected by an additional column Guard Cartridge Acclaim 120, C18 (5 μm , $2.1 \times 10 \text{ mm}$). The three-component mobile phase consisted of CH_3CN (A), 0.1% formic acid in CH_3CN (B) and water (C), which was delivered using a linear gradient at a constant flow rate equal to $0.3 \text{ ml}\cdot\text{min}^{-1}$. The gradient programme started with the following composition of the mobile phase: 50% A, 10% B and 40% C and its composition was linearly modified to reach 90% A, 10% B and 0% C after 9 min and then kept constant for 6.5 min. Conditioning the chromatographic column after separation took 9.5 min. The injection volume was equal to 10 μl and the temperature of the autosampler was set to 20 $^\circ\text{C}$.

The ESI mass spectra were recorded in the positive and full scan modes. The analytes were characterised and identified according to accurate measurements of masses of their parent and fragment ions using the MS/MS analysis and the ESI Compass 1.3 Data Analysis software (Bruker Daltonics, Germany). The parameters of the ESI source were set as follows: capillary voltage 4.0 kV, nebuliser pressure 1.2 bar, drying temperature 300 $^\circ\text{C}$ and dry gas flow rate of $8.0 \text{ dm}^3\cdot\text{min}^{-1}$. Nitrogen was used as the nebulising and collision gas.

2.6. Thermogravimetric analysis

The thermogravimetric analysis of SR 19 and SR 23 was performed using a Perkin Elmer Pyris-1 instrument. The sample of SR 19 (4.017 mg) was heated at temperatures from 30 $^\circ\text{C}$ up to 850 $^\circ\text{C}$. The sample of SR 23 (1.272 mg) was heated at temperatures from 30 $^\circ\text{C}$ up to 850 $^\circ\text{C}$. In both thermogravimetric analyses, the temperature was increased by 10 $^\circ\text{C}$ per minute.

3. Results and discussion

The chemical structures of the two red dyes, SR 19 and SR 23, that were used and studied are presented in Fig. 1. These compounds belong to a large group of commercially important azo dyes that have two $-\text{N}=\text{N}-$ functional groups that are substituted by aryl. They have a conjugated π double bond system due to which they can delocalise electrons throughout an entire molecule. Because they are also chromophores, they can absorb light in the UV/Vis region, the band position of which depends on the type, amount and substitution site of the auxochromes. Azo dyes usually have a trans configuration around the $-\text{N}=\text{N}-$ group [10]. Moreover, as was described in reference [33], SR 23 can exist as two keto tautomers, but the irradiation of light in the UV/Vis region causes isomerisation to a cis form. This trans-cis isomerisation is reversible both photochemically and thermally and

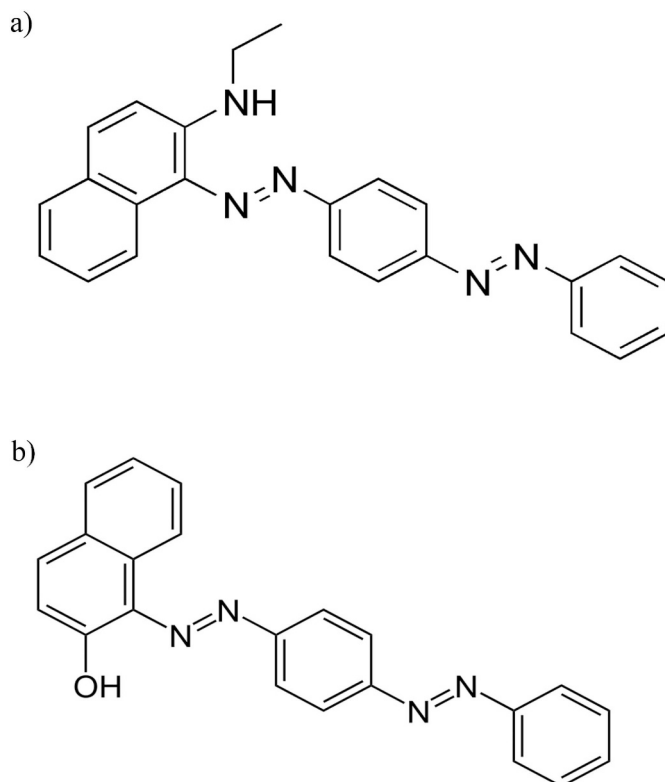


Fig. 1. Chemical structures of the two disazo dyes: a) Solvent Red 19 (N-Ethyl-1-((4-phenyldiazenyl)phenyl)diazenyl)naphthalen-2-amine) and b) Solvent Red 23 (1-(4-(Phenyldiazenyl)phenyl)azonaphthalen-2-ol).

induces remarkable changes in the properties of these dyes including differences in the respective absorption spectra [34,35].

3.1. Confirming the thermal stability of SR 19 and SR 23

The thermal decomposition of SR 19 is initiated at 205 $^\circ\text{C}$ (see Fig. 2a). The sample weight loss of about 75%, which was observed on the thermogram in the range of 205 $^\circ\text{C}$ and 292 $^\circ\text{C}$ (see Fig. 2b), could be associated with the loss of $\text{C}_{18}\text{H}_{18}\text{N}_4$. The lack of additional peaks on the thermogram suggests that there were no more thermal decomposition products. The decomposition of SR 23 was observed at 250 $^\circ\text{C}$, respectively (see Fig. 2c). The sample weight loss that was registered in the range of 250 $^\circ\text{C}$ and 315 $^\circ\text{C}$ (see Fig. 2d) indicates that there were two thermal degradation products with the potential structures $\text{C}_{10}\text{H}_{11}\text{ON}$ and $\text{C}_6\text{H}_5\text{NH}_2$. These two products underwent a further thermal decomposition in the range of 470 $^\circ\text{C}$ up to 640 $^\circ\text{C}$. The thermogravimetric analysis confirmed that both disazo dyes were thermally stable in normal exploitation and storage conditions. Therefore, the intensity of the colour fading in the samples that contained either SR 19 or SR 23 cannot be explained by their thermal decomposition.

3.2. Evaluating the effects of the UV-A irradiation, temperature, and duration of storage

In the course of the experiment, the samples that contained either SR 19 or SR 23 were stored in two climatic chambers and exposed to UV-A irradiation (factor A), temperature (factor B), and different durations of sample storage (factor C). All three factors were set at two levels (a low and a high level) following the two-level full factorial experimental design. Changes in the amount of dye in a sample as a result of the influence of the three factors were quantified based on the observed fading of the initial colour intensity. Therefore, the UV/Vis spectra were evaluated only in the visible range in order to evaluate the

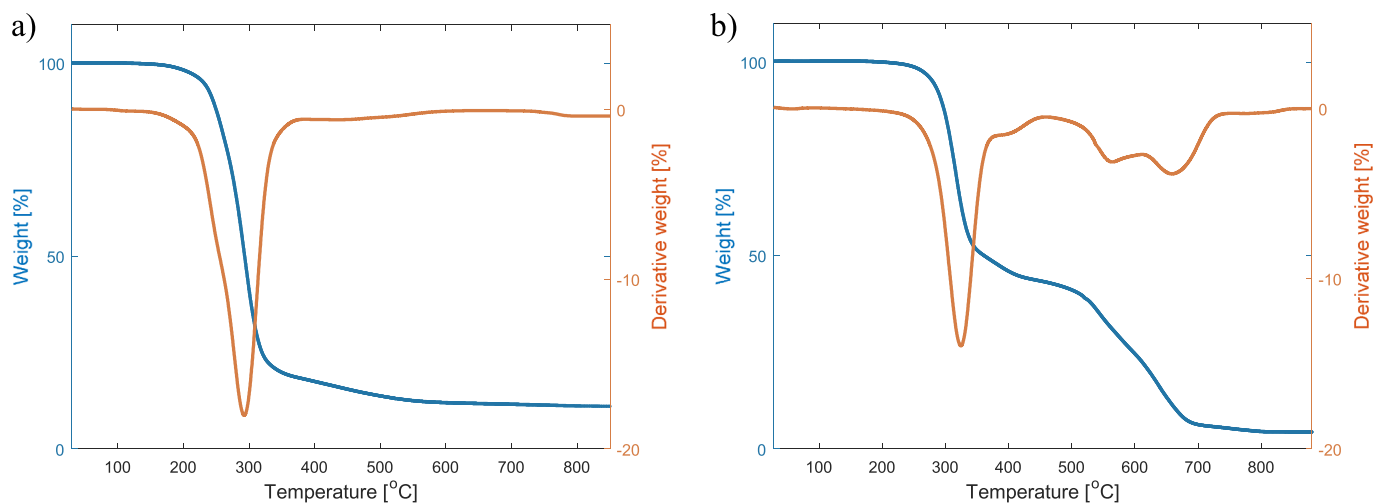


Fig. 2. The first derivative of weight loss expressed as a percentage (a red line) and weight loss expressed as a percentage (a blue line) in the function of temperature for a) SR 19 and b) SR 23. (For interpretation of the references to colour in this figure legend, the reader is referred to the web version of this article.)

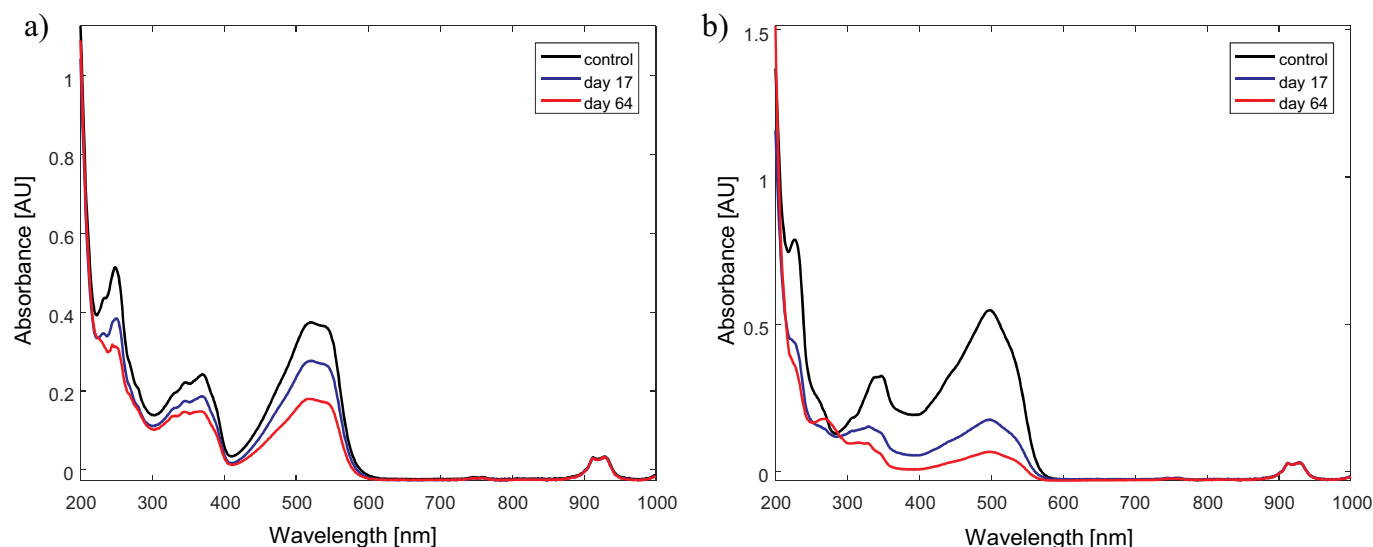


Fig. 3. The UV/Vis spectra that were recorded at the beginning of the experiment (black line), after 17 days (blue line) and after 64 days (red line) that describe the model mixtures that contained a) SR 19 and b) SR 23. (For interpretation of the references to colour in this figure legend, the reader is referred to the web version of this article.)

impact of the selected factors on the concentration of a given dye. The perception of colour by the human eye is limited to a spectral range between 380 and 630 nm. Fig. 3 presents the absorption UV/Vis spectra of the mixtures that contained either SR 19 or SR 23. The spectrum of the control mixture is indicated by the black line, whereas the spectra of the mixtures that were evaluated after 17 and 64 days are represented by blue and red lines, respectively.

Selective light absorption in the visible range is responsible for the colour intensity. The absorption spectra of the investigated diazo dyes were dependent on both their molar absorption coefficient and their concentrations. Therefore, the spectrophotometric method, which is recommended for determining the amount of dye and euromarker in fuel products [8] is based on monitoring the colour fading. To evaluate the decrease in the concentration of a dye over time, we adopted a similar response function as the one that is used in the recommended spectrophotometric method in the DoE. However, the active area of the spectrum that was used to monitor the sample colour was limited to only the visible region. The magnitude of the changes in sample colour was expressed as the difference between the area under the spectrum that was calculated for the control sample and the area under the

spectrum for the sample that was exposed to the three factors. The area under a given spectrum was integrated using the trapezoidal method [36]. Tables 1 and 2 list the settings of the three factors and the corresponding values of the response function for the mixtures that

Table 1

Design of experiment for mixtures containing SR 19 with values of the response function.

No.	UV-A		Temperature	Time	Interactions			Response
	A	B			AB	AC	BC	
1	-1	-1	-1	+1	+1	+1	36.90	
2	-1	+1	-1	-1	+1	-1	37.50	
3	+1	+1	-1	+1	-1	-1	28.24	
4	+1	-1	-1	-1	-1	+1	27.38	
5	-1	-1	+1	+1	-1	-1	39.94	
6	-1	+1	+1	-1	-1	+1	37.30	
7	+1	+1	+1	+1	+1	+1	18.72	
8	+1	-1	+1	-1	+1	-1	17.56	
Effect	-14.94	-0.005	-4.12	1.02	-5.54	-0.74		

Table 2
Design of experiment for mixtures containing SR 23 with values of the response function.

No.	UV-A			Temperature			Response
	A	B	C	AB	AC	BC	
1	-1	-1	-1	+1	+1	+1	39.61
2	-1	+1	-1	-1	+1	-1	39.92
3	+1	+1	-1	+1	-1	-1	17.40
4	+1	-1	-1	-1	-1	+1	20.13
5	-1	-1	+1	+1	-1	-1	42.54
6	-1	+1	+1	-1	-1	+1	40.46
7	+1	+1	+1	+1	+1	+1	3.74
8	+1	-1	+1	-1	+1	-1	12.13
Effect	-27.28	-3.22	-4.55	-2.34	-6.28	-2.01	

contained either SR 19 or SR 23. Values ‘-1’ and ‘+1’ denote the ‘low’ and ‘high’ levels of the factors and their possible interactions.

An analysis of experimental results proved that the colour intensity of the samples did indeed fade over time. However, this was only valid when the samples were exposed to the UV-A radiation. The control samples, which were not irradiated during the experiment, preserved their colour intensity. The most significant decrease in the colour intensity of the samples was directly proportional to the value of the respective response function. An analysis of the response values indicated that for the samples that contained either SR 19 or SR 23, the most significant decrease in the colour intensity was detected when a sample was exposed to the UV-A radiation over time. Thus, the most influential and dominant factor was determined to be the UV-A irradiation. This observation was confirmed by the magnitudes of the effects for the individual factors and their combinations, which are visualised in the respective normal probability plots in Fig. 4 in which all of the experiments are ranked according to the values of the individual effects and their combinations. Once the major factors and/or their combinations were close to a straight line (see the grey dotted line in Fig. 4a and b), their impact on the response function was relatively low and, therefore, they had a negligible influence on the colourfastness. On the other hand, the influence of a given factor and/or its combinations on the response value increased when the value of the corresponding effect was more distant from this line. For the model mixtures that were prepared with SR 19 in the first experiment, it was possible to conclude that factor A (the UV-A radiation) did indeed contribute substantially to

colour fading. The analysis of variance, ANOVA, also confirmed that only the variance, which is explained by factor A is significantly higher than the variance in the residuals (confidence level 95%).

The magnitudes of effects for factor C (time of sample storage) and its interaction with factor A (the UV-A irradiation and time of sample storage) are also pronounced, but not statistically significant as the effect of factor A, as depicted in Fig. 4a and confirmed by the ANOVA. The fading of colour for samples which contain SR 23 also depends mainly on the effect of factor A (the UV-A irradiation, Fig. 4b). The remaining factors are statistically insignificant as confirmed by the ANOVA. Comparing the magnitude of effect A in the other two experiments, either with SR 19 or SR 23, the dynamics of colour fading is much faster in the latter. Absolute changes in the area of spectrum in the visible range for a control sample and for a sample that exhibits the largest colour fading after 64 days, confirm that the colour fading for SR 23 is eight times faster than for SR 19. Therefore, one can conclude that SR 23 is indeed less chemically stable due to its higher instability to UV-A radiation than SR 19. It is relevant to point out that the chemical stability of SR 23 also decreased due to the effect of temperature. The colour fading of the samples with SR 23 was faster at higher temperature compared to samples with SR 19.

Two additional tables with ANOVA results, summarizing experiments carried out for SR 19 and SR 23, were provided in the Supplementary material.

Bearing in mind the chemical structures of the two disazo dyes, variations in the colour intensity are only possible when the configuration of dye molecule changes. By analogy to the conformation changes of structurally similar azobenzene compounds that contain only one azo chromophore [35], the photoisomerisation of disazo dyes that were studied is natural. Therefore, samples contained cis- and trans- isomers. The photoisomerisation of azobenzene, which is induced by UV-A radiation and/or temperature, as was described in detail in reference [16], is reversible. Isomer trans- is more stable than isomer cis- and therefore, its amount in a mixture is expected to be larger. The absorption spectra of cis- and trans-azobenzene indicate that the photoisomerisation of azobenzene indeed had an impact on the sample colour. However, both isomers absorb light in the visible range [37].

Nonetheless, photoisomerisation is a reversible process and cannot result in a permanent loss of the sample colour [10]. Compared to azobenzene, the SR 19 and SR 23 dyes, which are more structurally advanced forms, contain the chromophore and auxochrome groups. Their presence favours the transition of absorption towards longer

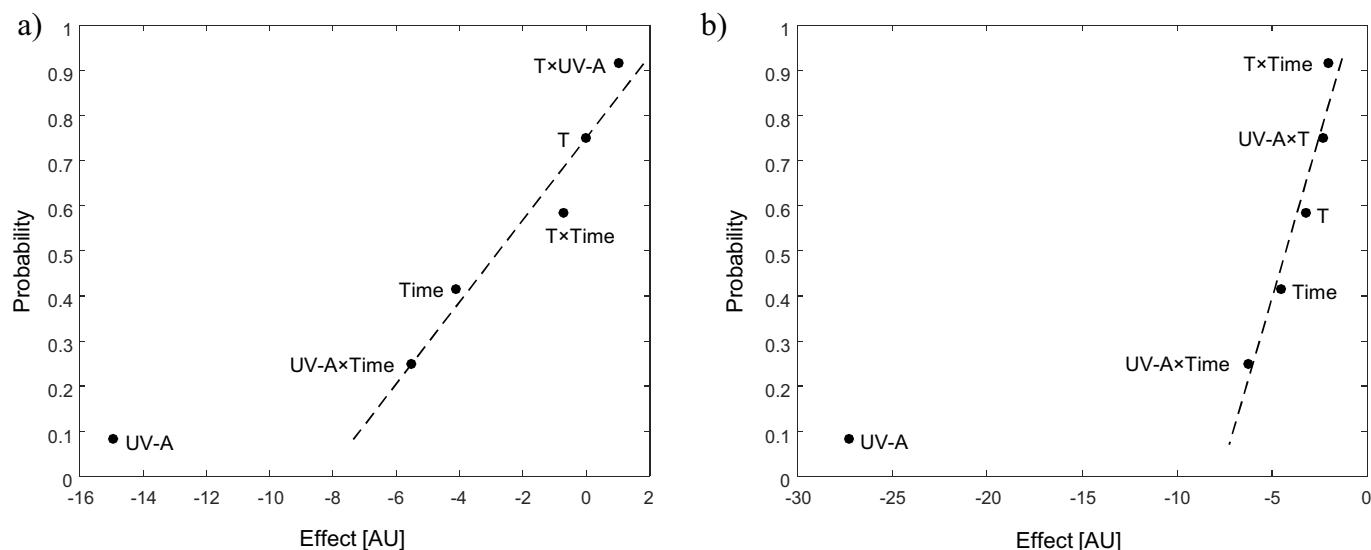


Fig. 4. The normal probability plot of the effects and their interactions for mixtures that contained a) SR 19 and b) SR 23. The three factors that were investigated in the experiments correspond to the exposure to the UV-A irradiation (A), temperature (B) and the duration of sample storage (C).

wavelengths. The chemical structures of the SR 19 and SR 23 dyes have two disazo groups and, depending on the energy levels, they may exist as different configuration isomers. Thus, a relatively simple photoisomerisation mechanism does not explain the irreversible loss of colour in the samples that contained one of these two dyes.

The differences in the colour and colour intensity of a sample can be attributed directly to configuration changes of the auxochromes that are present in a dye molecule and some possible structural modifications of its chromophores. However, the irreversible modification or fading of colour, and eventually, its permanent loss involves a functional inhibition of the chromophores in a sample. These two scenarios are possible only when a given molecule is prone to a chemical modification and/or is amenable to chemical degradation. In the case of the two disazo dyes being studied, both scenarios are likely to happen and can help to understand why the sample colour fades. This hypothesis was confirmed in (i) a detailed analysis of the molecular structure of both dyes from the perspective of photochemistry, (ii) an analysis of the fluorescence excitation-emission spectra and (iii) the changes that were detected in the composition of the samples, which were described by their respective chromatographic profiles.

While the Vis spectra of the samples confirmed the general tendency that can be spotted even by the eyes – the colour of the samples faded over time, the corresponding UV spectra, the fluorescence excitation-emission spectra and the chromatographic profiles provide substantial evidence that over time different degradation products are formed. Because the changes in the chemical composition of the samples were observed only when they were exposed to UV-A irradiation over a long period of time, in our opinion, the mechanism of the photo-induced degradation of SR 19 and SR 23 is the most probable and dominant one.

The intensity and/or the shape of the UV spectra changed over time, which indicates some instability of the chemical composition of the mixtures. This observation was true for both of the experiments that were carried out independently. Interestingly, the intensities of the UV spectra that described the SR 19 mixtures decreased over time systematically in the entire UV spectral range. The shape of spectra that were recorded for these mixtures 17 and 64 days after the beginning of the experiment resembled the shape of the spectrum for the control sample (see Fig. 3a). This observation drew our attention to the fact that a decrease in the concentrations of the mixture constituents had a significant influence on the shape of the corresponding spectrum. However, the pattern of the changes in the UV spectra that described the SR 23 mixtures was very different. In this case, the UV spectra shapes were noticeably modified compared to the shape of the control spectrum, which supports the conclusion that new degradation products are formed over time. The most extensive spectrum change was observed after 64 days and was visible up to 300 nm (see Fig. 3b).

The fluorescence spectroscopy had a remarkably low sensitivity compared to the UV/Vis spectroscopy and this property was highly valued in our study because some possible degradation products of SR 19 and SR 23 can have very low concentrations. On the other hand, in order to detect potential degradation products successfully using fluorescence spectroscopy, the chemical substances should contain fluorophores, i.e., specific groups that can emit fluorescence when they are excited. Different fluorophores are excited with beams of electromagnetic radiation at a characteristic wavelength. Therefore, the excitation-emission spectra enable a more comprehensive analysis of the changes in the chemical composition of the samples and increase the possibility of detecting several compounds simultaneously when some specific requirements are met. Fig. 5 illustrates the variations in the total fluorescence spectra of the control samples that contained either SR 19 or SR 23 and the total fluorescence spectra that were measured 17 and 64 days after the beginning of the experiment. These are displayed as colour maps in which individual measurements are coded by different colours with the intensities that were proportional to their magnitudes.

In general, the excitation-emission spectra of the mixtures and their

changes over time were very different. Regarding the SR 19 mixtures, the most pronounced differences in their excitation-emission spectra indicated quantitative and qualitative changes in their chemical composition. These changes were far more noticeable after 17 than after 64 days (compare Fig. 5a, b and c). The peak with the maximum intensity of fluorescence around 380 nm in the emission spectrum became much smaller compared to the control sample. Moreover, the presence of compound(s) that were absent in the control sample was confirmed. Their fluorophores were excited in the spectral range between 290 nm and 310 nm and emitted fluorescence that led to a broad peak in the emission spectrum with a maximum intensity of around 350 nm. Regarding the SR 23 mixtures, the most substantial differences in the excitation-emission spectra were noticed 17 days after the beginning of the experiment (see Fig. 5d and e). The excitation-emission spectra for the control sample were noisy and had very low intensities. After 17 days, it was possible to observe two intensive spots, which suggests that there were some qualitative changes in the chemical composition of the mixture. As is illustrated in Fig. 5f and g, the amount of the respective degradation products increased over time.

3.3. Interpreting the chromatographic profiles that were obtained from the model mixtures

Although the excitation-emission spectra suggested changes in chemical composition of the studied mixtures, it was difficult to identify the number of mixture components and potential degradation products. Although this can be done using high-performance chromatography with the UV/Vis and mass spectrometry detection, it can be a very challenging analytical task because commercially available dyes could contain different numbers of impurities [38,39].

Fig. 6a and b display the chromatograms for the SR 19 or SR 23 mixtures at different time points of the experiment. All of them were registered by measuring the absorption of the eluate at 500 nm. In the upper panel of Fig. 6, the chromatograms with black lines illustrate the control samples, while the chromatographic profiles with blue and red lines describe the content in the samples 17 and 64 days after the beginning of the experiment. The chromatographic profiles confirmed the decrease in the concentrations (two-fold) of the studied dyes 64 days after the beginning of the experiment. In addition to the major component, which eluted from the SR 19 mixture at around 14.2 min or around 12.6 min for the SR 23 mixture, respectively, there are several peaks more in chromatograms. Most likely, these can be associated with some impurities that were present in the reagent or other degradation products. These are two possible sources because the chromatogram of the solvent (n-heptane) did not contain any additional peaks. The presence of potential impurities in mixtures led us to focus on identifying the chemical differences in the mixture samples with respect to the chemical content of the control sample 17 and 64 days after the beginning of the experiment.

The level of impurities, which was estimated using the chromatographic profile of a control SR sample at 500 nm, was below 2.50%. Table 3 presents information about the eleven chromatographic peaks that were recorded in the analysed mixtures along with the m/z value of the precursor ion that had originated from the compound that was detected in a given peak at the beginning of the experiment and after 17 and 64 days.

Most of the peaks were separated well, which enabled the chemical differences in the mixtures to be analysed with respect to the control sample. When the three chromatograms are compared, it can be concluded that the dye, which is the most significant component, underwent the most noticeable changes (see Fig. 6a, peak no. 11).

From the quantitative data in Table 3, it can be concluded that the amount of dye decreased considerably by a factor of 1.78 during the course of the experiment. While the concentrations of some compounds decreased over time, the levels of others increased and some compounds were present only in the middle phase of the experiment or

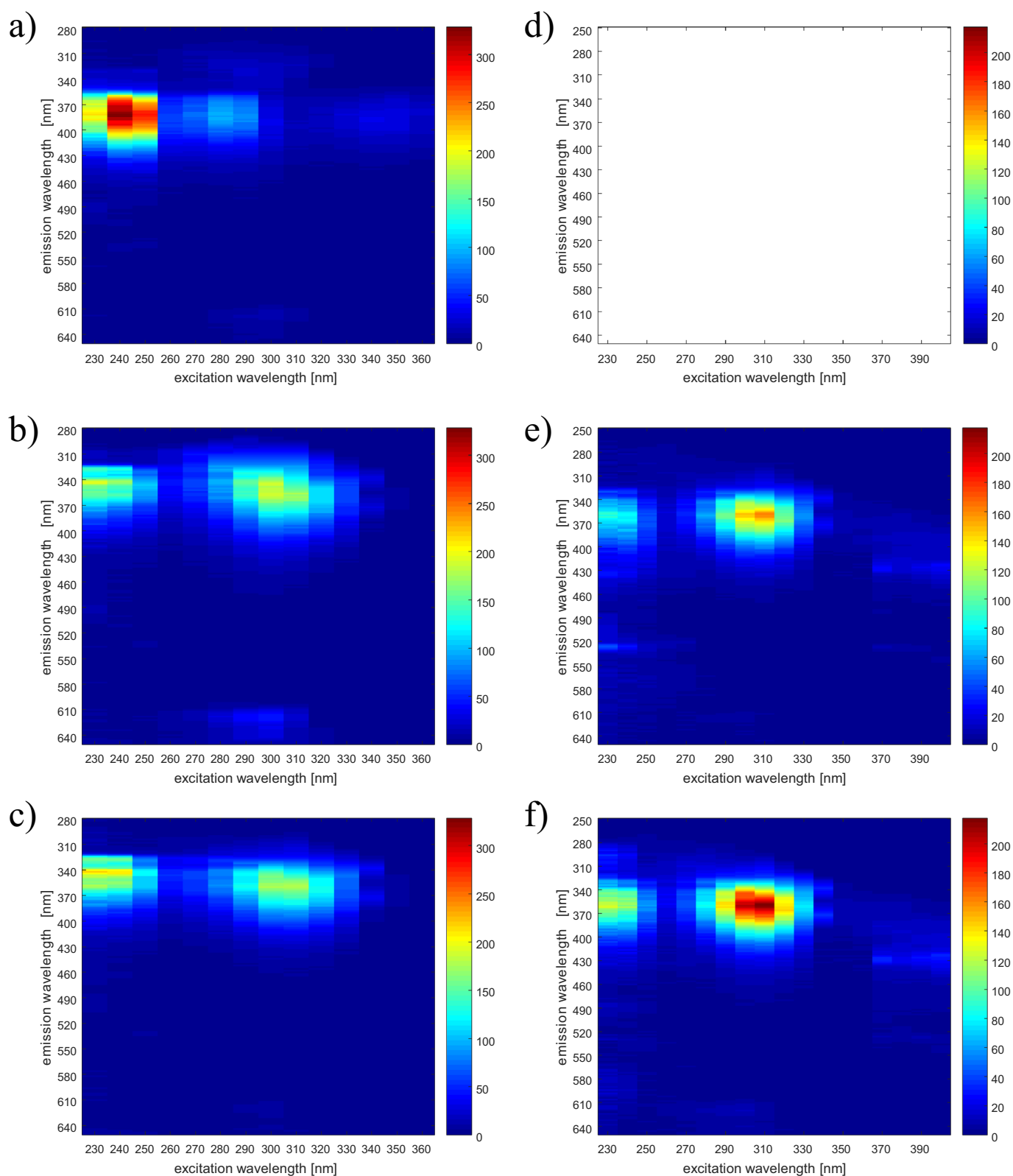


Fig. 5. The excitation-emission spectra of the model mixtures that contained either SR 19 (a–c) or SR 23 (d–f) that were recorded at the beginning of the experiment, after 17 days and 64 days, respectively.

were eventually undetectable. These quite diverse patterns of system behaviour indicate the dynamics of the photo fading process. To some extent, it can be argued that the decrease in the dye concentration that was observed over time might be associated with its degradation. In fact, the concentration of the other components must simultaneously

increase and/or new components should be detected. The decrease in the concentration of SR 19 was accompanied by an increase in the amounts of compounds nos. 3, 5, 7 and 9 in the mixtures after 17 days. It is important to note that these four compounds were not detected in the control sample and therefore their presence can be interpreted as

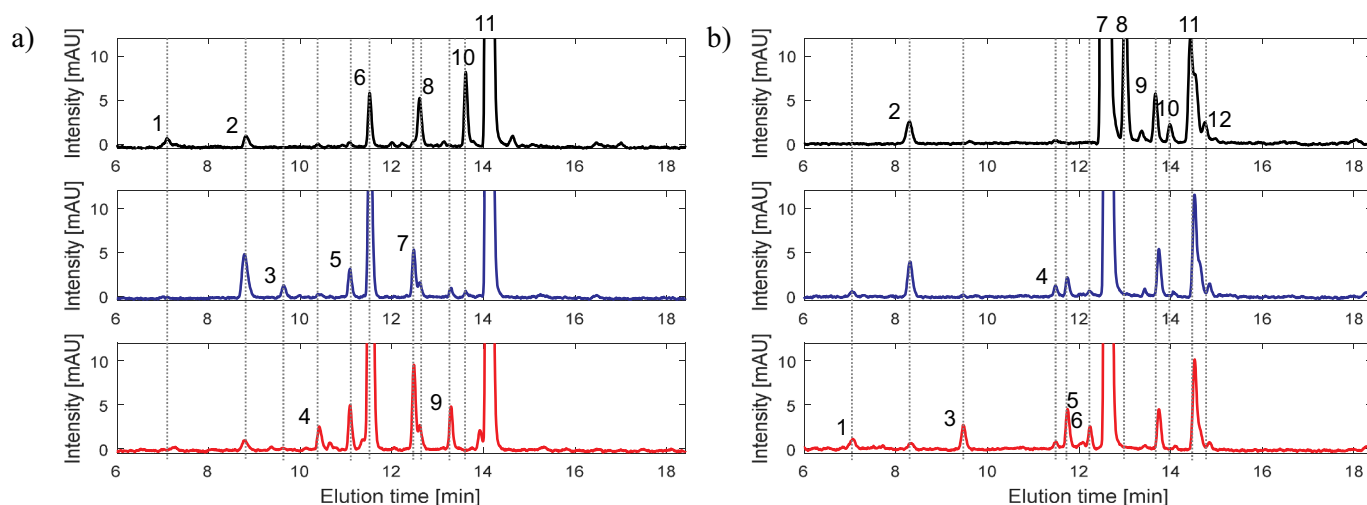


Fig. 6. The HPLC chromatograms that reveal the changes in the chemical composition of the model mixtures that contained a) SR 19 and b) SR 23 that were observed at the beginning of the experiment (the upper panel), after 17 days (the middle panel) and after 64 days (the lower panel). The chromatograms were recorded using a UV/Vis detector to measure the absorbance of the eluate at 500 nm.

Table 3

Eleven chromatographic peaks that were identified in model mixtures containing SR 19 (along with approximate elution time, the m/z value of the precursor ion originating from compound detected in a given peak, and the corresponding peak areas). Model mixtures were incubated in elevated temperature and exposed to the UV-A irradiation and chromatographed after 0, 17, and 64 days since the beginning of the experiment. Peak no. 11 corresponds to major component – SR 19.

Peak no.	Elution time [min]	Precursor ion (m/z)	Day 0	Day 17	Day 64
1	7.09	291.15	0.065	0	0
2	8.81	378.16	0.103	0.680	0.535
3	9.64	394.16	0	0.110	0
4	10.41	321.13	0	0	0.224
5	11.08	378.16	0	0.286	0.420
6	11.51	352.14	0.462	2.667	12.421
7	12.48	394.16	0	0.463	0.853
8	12.60	326.16	0.479	0	0
9	13.29	296.17	0	0.079	0.429
10	13.61	380.18	0.678	0.037	0
11	14.12	380.18	80.113	57.785	44.915

the result of the degradation of the dye and/or other mixture compounds that are amenable to photodegradation. The most substantial increase in concentration was recorded for compound no. 6. After 17 days, its concentration was 5.77 times higher compared to the control sample and was 26.89 times higher after 64 days. The concentrations of compounds nos. 5, 6, 7 and 9 increased during the 17-day experiment and increased even more after 64 days. On the other hand, compounds nos. 1, 8 and 10 were eventually not recorded over time. The most rapid change in the concentration level was observed for compound no. 10. It is likely that the chemical stability of these compounds was affected to a large extent by the UV-A irradiation as this was also observed for SR 19. Another probable explanation anticipates the further involvement of these compounds in other chemical reactions. For instance, compound no. 3 was detected only in the interim phase of the experiment, which suggests that it might be an intermediate product. However, in order to successfully confirm this hypothesis, some additional experiments and modifications (or further development) of the analytical method are required. From the analysis of the collected chromatographic profiles and after examining the respective quantitative data, only a partial explanation of changes in SR 19 was possible. Namely, the decrease in the peak area of the major sample component was not accompanied by an adequate increase in the peak areas of the other compounds. Of course, this conclusion holds

true for the chromatograms that were registered using a specific chromatographic system, method of detection and chromatographic conditions. The changes that were observed for compounds nos. 7 and 8 are also interesting. These two compounds coeluted, which is illustrated by the chromatogram in Fig. 6a. After 17 days, compound no. 8 was not detected in a mixture (at a given detection wavelength and chromatographic conditions), while the concentration of compound no. 7 increased ca. 1.84 times.

An analysis of the chromatograms for the model SR 23 mixtures suggested a dynamic change in their chemical compositions over time. Twelve peaks, which were recorded at the beginning of the experiment as well as after 17 and 64 days, were identified (see the three panels in Fig. 6b and Table 4) in the chromatograms. They represent the compounds that behaved differently during the course of the experiment. The SR 23 from the control model mixture eluted at 12.61 min and yielded the most intensive peak (peak area equal to 174.744), which is shown in the chromatogram in the upper panel of Fig. 6b. Moreover, there were at least eight minor peaks in the chromatogram that represented impurities because their relative concentrations with respect to the concentration of SR 23 ranged between 0.14% and 1.11%. The amount of the major sample component (SR 23) decreased considerably

Table 4

Twelve chromatographic peaks that were identified in model mixtures containing SR 23 (along with approximate elution time, the m/z value of the precursor ion originating from compound detected in a given peak, and the corresponding peak areas). Model mixtures were incubated in elevated temperature (30 °C) and exposed to the UV-A irradiation and chromatographed after 0, 17, and 64 days since the beginning of the experiment. Peak no. 7 corresponds to major component – SR 23.

Peak no.	Elution time [min]	Precursor ion (m/z)	Day 0	Day 17	Day 64
1	7.08	291.15	0	0.069	0.110
2	8.29	353.14	0.465	0.440	0.126
3	9.47	408.13	0	0	0.341
4	11.48	383.27	0	0.127	0.066
5	11.74	347.31	0	0.247	0.437
6	12.24	351.20	0	0.050	0.228
7	12.61	353.13	174.744	105.547	75.901
8	13.00	383.31	1.937	0	0
9	13.66	560.25	0.593	0.536	0.486
10	13.98	429.16	0.250	0.050	0.027
11	14.43	380.18	1.552	1.218	1.085
12	14.76	381.17	0.500	0.159	0.058

over time by a factor of 2.3. Compared to the decrease of SR 19 64 days after the beginning of the experiment, it can be pointed out that SR 23 was more susceptible to photo fading, and therefore, was less stable when it was exposed to the UV-A irradiation. This observation was also confirmed by an analysis of fluorescence and Vis spectra. Like the SR 19 mixtures, the pattern of chemical changes in the SR 23 mixtures was also similar. Namely, some compounds were always present at each step of the experiment, the concentration some of them decreased and some became more pronounced or were detected later. For example, compound no. 2 had rather negligible concentration differences in the mixtures at the beginning of the experiment and after 17 days. However, its concentration decreased sharply by almost 3.7 times after 64 days. Similar behaviour was observed for compound no. 9. Together with the main mixture component, the concentrations of compounds nos. 10–12 steadily decreased over the 64 days. Compound no. 8 was not detected in the chromatographed mixture after 17 days, which makes it a potential marker of colour fading due to fuel laundering. On the other hand, the detection of compound no. 3 was possible only when a mixture was irradiated at least 17 days. Compounds nos. 1, 5 and 6 were absent in the initial mixture, but their concentrations increased over time.

Additional figures, submitted along with the article, are mass spectra of the possible degradation products of SR 19 and SR 23, and they correspond to possible structures listed in [Appendix 1](#) and [Appendix 2](#).

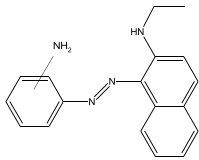
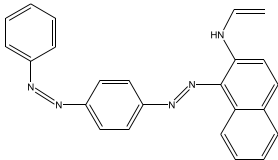
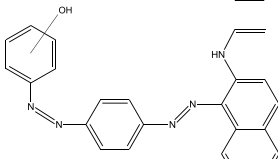
4. Conclusions

In this study, we demonstrated that the two red disazo dyes, SR 19 and SR 23, which are frequently used as excise duty components to label fuel products, can be chemically unstable depending on the storage conditions. The results of two designed experiments proved that UV-A irradiation affected their chemical stability the most. Because of the two disazo bonds that are present in the chemical structures, both dyes are amenable to photoisomerisation. Therefore, they exist as different conformation isomers. However, the extensive irradiation of a mixture with a given dye led to a permanent loss of colour over time, which was associated with the destruction of its chromophores and resulted in a specific sample colour. This hypothesis was confirmed by the differences in the chemical composition of samples that were detected using the spectroscopic and chromatographic techniques. The

Appendix A

Appendix 1

Potential structures of identified compounds in the studied mixtures based on the HPLC analysis combined with the interpretation of the corresponding MS and MS/MS spectra. Peak no. 11 is the major component – SR 19. The corresponding mass spectra are provided in the 'Supplementary material' section.

Peak no.	Elution time [min]	Precursor ion (m/z)	Potential structures
1	7.09	291.15	
2	8.81	378.16	
3	9.64	394.16	

(continued on next page)

chromatograms and the respective mass spectra indicated that the chemical composition of the mixtures changed dynamically over time. The chemical structures of several possible degradation products are proposed and are provided in the [Appendix](#). We anticipate that the final effect was the result of photoinduced degradation of dyes that were studied in the experiments as well as the possibility that they can self-sensibilise due to the intrinsic properties of molecules. The quantitative results indicate that SR 23 is less chemically stable than SR 19 because the colour of the model SR 23 mixture faded much faster (ca. eight-fold). To summarise, monitoring the amount of excise duty components in fuel products using the recommended spectroscopic technique is insufficient to confirm illegal attempts at fuel laundering.

CRediT authorship contribution statement

M. Daszykowski: Conceptualization, Methodology, Funding acquisition, Project administration, Writing - review & editing. **J. Orzel:** Investigation, Visualization. **I. Stanimirova:** Methodology, Software, Formal analysis, Visualization, Writing - review & editing. **A. Poliwoda:** Investigation, Resources. **D. Prukala:** Investigation, Resources. **P. Mlynarz:** Investigation, Resources.

Declaration of competing interest

The authors declare that they have no known competing financial interests or personal relationships that could have appeared to influence the work reported in this paper.

Acknowledgements

MD, JO, IS, AP, DP, and PM would like to acknowledge the support of the National Science Centre, Poland (research grant no. 2014/13/B/ST4/05007).

Mrs. Patrycja Ziemianek and Mr. Michał Gajewski are kindly acknowledged for their support in the early phase of research.

Dr. Slawomir Maslanka from the Institute of Chemistry, University of Silesia in Katowice, Poland, is kindly acknowledged for his assistance in the thermogravimetric analysis of the two disazo dyes that were investigated in this study.

Appendix 1 (continued)

Peak no.	Elution time [min]	Precursor ion (m/z)	Potential structures
4	10.41	321.13	
5	11.08	378.16	
6	11.51	352.14	
7	12.48	394.16	
8	12.60	326.16	
9	13.29	296.17	
10	13.61	380.18	
11	14.12	380.18	

Appendix 2

Potential structures of identified compounds in the studied mixtures based on the HPLC analysis combined with the interpretation of the corresponding MS and MS/MS spectra. Peak no. 7 corresponds to major component – SR 23. The corresponding mass spectra are provided in the ‘Supplementary material’ section

Peak no.	Elution time [min]	Precursor ion (m/z)	Potential structures
1	7.08	291.15	
2	8.29	353.14	

(continued on next page)

Appendix 2 (continued)

Peak no.	Elution time [min]	Precursor ion (m/z)	Potential structures
3	9.47	408.13	
4	11.48	383.27	
5	11.74	347.31	-
6	12.24	351.20	-
7	12.61	353.13	
8	13.00	383.31	-
9	13.66	560.25	-
10	13.98	429.16	-
11	14.43	380.18	
12	14.76	381.17	

Appendix B. Supplementary data

Supplementary data to this article can be found online at <https://doi.org/10.1016/j.fuproc.2020.106465>.

References

- [1] J. Orzel, M. Daszykowski, Recent trends in the use of liquid fuel taggants and their analysis, *TrAC Trends Anal. Chem.* 87 (2017) 98–111, <https://doi.org/10.1016/j.trac.2016.11.010>.
- [2] Dz.U.2019.1822: Znakowanie i barwienie wyrobów energetycznych, (2019).
- [3] H. Emteborg, S. Elordui-Zapatarietxe, Evaluation of the performance of the short-listed candidate markers regarding the technical requirements, Publication Office of the European Union, European Union, 2017.
- [4] B. Krakowska, I. Stanimirova, J. Orzel, M. Daszykowski, I. Grabowski, G. Zaleszczyk, M. Sznajder, Detection of discoloration in diesel fuel based on gas chromatographic fingerprints, *Anal. Bioanal. Chem.* 407 (2015) 1159–1170, <https://doi.org/10.1007/s00216-014-8332-4>.
- [5] J. Orzel, M. Daszykowski, I. Grabowski, G. Zaleszczyk, M. Sznajder, Identifying the illegal removal from diesel oil of certain chemical markers that designate excise duty, *Fuel* 117 (2014) 224–229, <https://doi.org/10.1016/j.fuel.2013.09.029>.
- [6] J. Orzel, B. Krakowska, I. Stanimirova, M. Daszykowski, Detecting chemical markers to uncover counterfeit rebated excise duty diesel oil, *Talanta* 204 (2019) 229–237, <https://doi.org/10.1016/j.talanta.2019.05.113>.
- [7] V.B. Croud, C.A. Marchant, P. Maltas, L. Hecht, R. Douglas, Criminal removal of fuel markers by distillation, *Fuel Process. Technol.* 144 (2016) 341–347, <https://doi.org/10.1016/j.fuproc.2015.12.005>.
- [8] PN-C-04426:2013-07, Ciekłe przetwory naftowe - spektrofotometryczne metody oznaczania znacznika Solvent Yellow 124 oraz czerwonego i niebieskiego barwnika w lekkich olejach opałowych i olejach napędowych, (2013).
- [9] J. Lorens-Lezon, A. Lezon, A. Stepien, Wpływ promieniowania słonecznego na trwałość znacznika Solvent Yellow 124 oraz barwnika Solvent Red 19 w lekkich

- olejach opałowych, *Przemysł Chemiczny* 93 (2014) 1418–1421, <https://doi.org/10.12916/przemchem.2014.1418>.
- [10] H.M.D. Bandara, S.C. Burdette, Photoisomerization in different classes of azobenzene, *Chem. Soc. Rev.* 41 (2012) 1809–1825, <https://doi.org/10.1039/c1cs15179g>.
- [11] H. Lachheb, E. Puzenat, A. Houas, M. Ksibi, E. Elaloui, C. Guillard, J.-M. Herrmann, Photocatalytic degradation of various types of dyes (Alizarin S, Crocein Orange G, Methyl Red, Congo Red, Methylene Blue) in water by UV-irradiated titania, *Appl. Catal. B Environ.* 39 (2002) 75–90, [https://doi.org/10.1016/S0926-3373\(02\)00078-4](https://doi.org/10.1016/S0926-3373(02)00078-4).
- [12] R. Podsiadły, J. Sokołowska, Photostability of a range of azobenzene dyes and their benzothiazolyl analogues in the presence of air, *Color. Technol.* 119 (2003) 341–344, <https://doi.org/10.1111/j.1478-4408.2003.tb00195.x>.
- [13] J. Qu, B. Liu, J. He, Photofading mechanisms of azo dye in its azo and hydrazone forms under UV irradiation, *J. Chem. and Pharm. Res.* 6 (2014) 1149–1154.
- [14] P. Bortolus, S. Monti, A. Albini, E. Fasani, S. Pietra, Physical quenching and chemical reaction of singlet molecular oxygen with azo dyes, *J. Organomet. Chem.* 54 (1989) 534–540, <https://doi.org/10.1021/jo00264a006>.
- [15] L.M.G. Jansen, I.P. Wilkes, F. Wilkinson, D.R. Worrall, The role of singlet molecular oxygen in the photodegradation of 1-arylozo-2-naphthols in methanol and on cotton, *J. Photochem. Photobiol. A Chem.* 125 (1999) 99–106, [https://doi.org/10.1016/S1010-6030\(99\)00095-7](https://doi.org/10.1016/S1010-6030(99)00095-7).
- [16] Z. Morita, S. Hada, A semiempirical molecular orbital study on the reaction of an aminopyrazolonyl azo dye with singlet molecular oxygen, *Dyes Pigments* 41 (1999) 1–10, [https://doi.org/10.1016/S0143-7208\(98\)00038-2](https://doi.org/10.1016/S0143-7208(98)00038-2).
- [17] P. Ball, C.H. Nicholls, The role of azo-hydrazone tautomerism in the photofading of 1-phenylazo-4-naphthol in polymer substrates, *Dyes Pigments* 5 (1984) 437–455, [https://doi.org/10.1016/0143-7208\(84\)80036-4](https://doi.org/10.1016/0143-7208(84)80036-4).
- [18] M.A. Rauf, M.A. Meetani, S. Hisaindee, An overview on the photocatalytic degradation of azo dyes in the presence of TiO₂ doped with selective transition metals, *Desalination*. 276 (2011) 13–27, <https://doi.org/10.1016/j.desal.2011.03.071>.
- [19] K.M. Reza, A. Kurny, F. Gulshan, Parameters affecting the photocatalytic degradation of dyes using TiO₂: a review, *Appl Water Sci* 7 (2017) 1569–1578, <https://doi.org/10.1007/s13201-015-0367-y>.
- [20] M.A.I. Molla, I. Tateishi, M. Furukawa, H. Katsumata, T. Suzuki, S. Kaneco, Photocatalytic decolorization of dye with self-dye-sensitization under fluorescent light irradiation, *ChemEngineering* 1 (2017) 8, <https://doi.org/10.3390/chemengineering1020008>.
- [21] T. Aarhi, P. Narahari, G. Madras, Photocatalytic degradation of Azure and Sudan dyes using nano TiO₂, *J. Hazard. Mater.* 149 (2007) 725–734, <https://doi.org/10.1016/j.jhazmat.2007.04.038>.
- [22] X.-R. Xu, H.-B. Li, W.-H. Wang, J.-D. Gu, Degradation of dyes in aqueous solutions by the Fenton process, *Chemosphere*. 57 (2004) 595–600, <https://doi.org/10.1016/j.chemosphere.2004.07.030>.
- [23] B.P. Vempatapu, P.K. Kanaujia, Monitoring petroleum fuel adulteration: a review of analytical methods, *TrAC Trends Anal. Chem.* 92 (2017) 1–11, <https://doi.org/10.1016/j.trac.2017.04.011>.
- [24] I. Barra, M.A. Mansouri, Y. Cherrah, M. Kharbach, A. Bouklouze, FTIR fingerprints associated to a PLS-DA model for rapid detection of smuggled non-compliant diesel marketed in Morocco, *Vib. Spectrosc.* 101 (2019) 40–45, <https://doi.org/10.1016/j.vibspec.2019.02.001>.
- [25] I. Barra, M.A. Mansouri, M. Bousrabat, Y. Cherrah, A. Bouklouze, M. Kharbach, Discrimination and quantification of Moroccan gasoline adulteration with diesel using Fourier transform infrared spectroscopy and chemometric tools, *J. AOAC Int.* 102 (2019) 966–970, <https://doi.org/10.5740/jaoacint.18-0179>.
- [26] H.O.M.A. Moura, A.B.F. Câmara, M.C.D. Santos, C.L.M. Morais, L.A.S. de Lima, K.M.G. Lima, L.S. de Carvalho, Advances in chemometric control of commercial diesel adulteration by kerosene using IR spectroscopy, *Anal. Bioanal. Chem.* 411 (2019) 2301–2315, <https://doi.org/10.1007/s00216-019-01671-y>.
- [27] R. Gotor, C. Tiebe, J. Schlichka, J. Bell, K. Rurack, Detection of adulterated diesel using fluorescent test strips and smartphone readout, *Energy Fuel* 31 (2017) 11594–11600, <https://doi.org/10.1021/acs.energyfuels.7b01538>.
- [28] W.F. Cordeiro Dantas, J.C. Laurentino Alves, R.J. Poppi, MCR-ALS with correlation constraint and Raman spectroscopy for identification and quantification of biofuels and adulterants in petroleum diesel, *Chemom. Intell. Lab. Syst.* 169 (2017) 116–121, <https://doi.org/10.1016/j.chemolab.2017.04.002>.
- [29] R. Leghrib, E. Ouacha, A. Zouida, B. Faiz, A. Amghar, Monitoring automobile fuel adulteration using ultrasound technique for environmental issues, *Measurement*. 150 (2020) 107004, <https://doi.org/10.1016/j.measurement.2019.107004>.
- [30] T. Tomić, S. Babić, M. Biošić, N.U. Nasipak, A.-M. Čížmek, Determination of the Solvent Blue 35 dye in diesel fuel by solid phase extraction and high-performance liquid chromatography with ultraviolet detection, *Dyes Pigments* 150 (2018) 216–222, <https://doi.org/10.1016/j.dyepig.2017.12.013>.
- [31] D.C. Montgomery, *Design and Analysis of Experiments*, 8 edition, Wiley, Hoboken, NJ, 2012.
- [32] R.G. Zepp, W.M. Sheldon, M.A. Moran, Dissolved organic fluorophores in southeastern US coastal waters: correction method for eliminating Rayleigh and Raman scattering peaks in excitation–emission matrices, *Mar. Chem.* 89 (2004) 15–36, <https://doi.org/10.1016/j.marchem.2004.02.006>.
- [33] B. Abbas, Y.T. Salman, Study of photo-induced dichroism in Sudan III doped in poly (methylmethacrylate) thin films, *Acta Phys. Pol. A* 127 (2015) 780–786, <https://doi.org/10.12693/APhysPolA.127.780>.
- [34] P. Bortolus, S. Monti, Cis-trans photoisomerization of azobenzene. Solvent and triplet donors effects, *J. Phys. Chem.* 83 (1979) 648–652, <https://doi.org/10.1021/j100469a002>.
- [35] E. Merino, M. Ribagorda, Control over molecular motion using the cis–trans photoisomerization of the azo group, *Beilstein J. Org. Chem.* 8 (2012) 1071–1090, <https://doi.org/10.3762/bjoc.8.119>.
- [36] N. Eggert, J. Lund, The trapezoidal rule for analytic functions of rapid decrease, *J. Comput. Appl. Math.* 27 (1989) 389–406, [https://doi.org/10.1016/0377-0427\(89\)90024-1](https://doi.org/10.1016/0377-0427(89)90024-1).
- [37] NIST Chemistry WebBook, <https://webbook.nist.gov/chemistry/> (accessed November 18, 2018).
- [38] J.Y. Hong, N.H. Park, K.H. Yoo, J. Hong, Comprehensive impurity profiling and quantification of Sudan III dyes by gas chromatography/mass spectrometry, *J. Chromatogr. A* 1297 (2013) 186–195, <https://doi.org/10.1016/j.chroma.2013.04.064>.
- [39] S.D. Harvey, G.W. Buchko, R.B. Lucke, C.W. Wright, A.M. Melville, A.J. Scott, B.W. Wright, The structure and purity of a reference dye standard used for quantification of C.I. Solvent Red 164 in fuels, *Dyes Pigments* 82 (2009) 307–315, <https://doi.org/10.1016/j.dyepig.2009.01.015>.